REVIEW PAPER

In-Vitro Screening methods of molecules for Alzheimer's Diseases

Hirak Shah[1], Dhwani Shah[2], Kunjal Vegad[3*]

[1]Assistant Professor, Department of Pharmaceutical Chemistry, Parul College of Pharmacy and Research, Parul University, Waghodia, Gujarat, India. hirakshah285@gmail.com
[2]Associate Professor, Department of Pharmaceutical Chemistry, Parul College of Pharmacy and Research, Parul University, Waghodia, Gujarat, India. shahdhwani57@gmail.com
[3*]Professor, Department of Pharmacognosy, Parul College of Pharmacy and Research, Parul University, Waghodia, Gujarat, India. Kunjalvegad11@gmail.com

Abstract
Alzheimer's disease (AD) is a progressive neurodegenerative disorder characterized by cognitive impairment, synaptic dysfunction, and neuronal loss. Despite significant research efforts, the development of effective disease-modifying therapies has been limited, underscoring the urgent need for innovative approaches in drug discovery. This review summarizes anti alzheimer's screening methods of molecules. The major pathogenic theories underlying Alzheimer's disease (AD) encompass several key mechanisms: cholinergic dysfunction, amyloid-beta accumulation, tau protein pathology, oxidative stress, metal ion imbalance, inflammation, and N-methyl-D-aspartate (NMDA) receptor dysregulation. Emphasis is placed on *in vitro* screening methods used to evaluate potential therapeutic agents targeting these pathways.
Various biochemical and cell-based assays are discussed, including acetylcholinesterase inhibition assays, fluorescence-based β-secretase (BACE-1) assays, tau fibrillization assays, antioxidant assays (ORAC), and metal chelation studies. Additionally, advanced cellular models such as primary neuronal cultures, human induced pluripotent stem cell-derived neurons, and immortalized cell lines are highlighted for studying excitotoxicity and neuroprotection. Techniques for measuring intracellular calcium levels and assessing blood–brain barrier integrity further support mechanistic evaluation. Overall, these *in vitro* methodologies provide essential tools for early-stage screening and optimization of multi-target-directed ligands, thereby facilitating the development of effective therapeutic strategies for AD.

Keywords: Alzheimer's disease; In vitro screening; Acetylcholinesterase; Amyloid-beta; Tau protein; NMDA receptor; Oxidative stress; Metal chelation; Neuroinflammation; Drug discovery
How To Cite This Article: Shah H, Shah D, Vegad K. In-Vitro Screening Methods Of Molecules For Alzheimer's Diseases. Int J Drug Deliv Technol. 2026;16(25s):969-977. Doi: 10.25258/ijddt.16.25s.113

1. INTRODUCTION

Alzheimer's disease (AD) is marked by degeneration of nervous tissue, that massively alters the mental capacity of patients. Dementia is a clinical manifestation of the neurodegenerative process and ultimately AD, which is linked to widespread impairments in neurotransmission and impairment of neuronal function in brain regions crucial to cognitive activities [1]. Though understanding pathological process and identifying biomarkers for diagnosis are key targets for the treatment of AD [2], still no effective pharmacological treatment available for prevention of advancement of disorder [3]. Therefore, it is critical to continue developing disease-modifying treatments that target the primary pathways of the illness in order to slow the emergence of structural and functional abnormalities in the central nervous system (CNS), which may lead to long-term improvements in cognitive functions [4].

It is necessary to develop new treatments to stop or postpone the emergence of symptoms, reduce the illness's progression, or enhance the behavioral and cognitive signs of AD.

All clinical studies evaluating pharmacological treatments for AD that were ongoing as of January 1, 2024, and Common Alzheimer's Disease Research Ontology (CADRO) was utilized to categorize the potential targets of upcoming treatments were shown in fig. 1 [5].

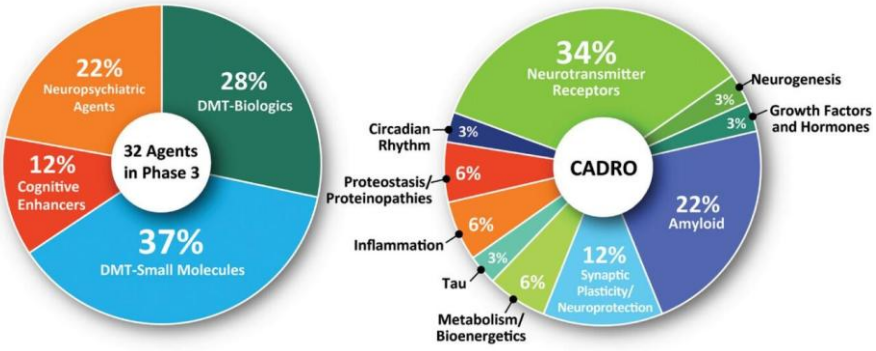

[Figure:1 Mechanisms of action of agents in Phase 3 Alzheimer clinical trials as classified using 4 categories of therapeutic purpose (left) or the Common Alzheimer's Disease Research Ontology (CADRO) approach (right)]

2. PATHOGENESIS

2.1. Cholinesterase Hypothesis

According to cholinergic hypothesis, cholinergic activity disruption in the brains of healthy and dementia patients may contribute to memory loss and related cognitive impairment; thus, cholinergic function reconstruction may be able to lessen the severe loss of cognitive function [6]. The activity of the cholinergic system was evaluated by choline acetyl transferase (ChAT) and acetylcholinesterase (AChE) [7]. The study showed that the Ach, ChAT and AChE in the brain of AD patients showed a continuous decline [8].

2.1.1. Acetylcholinesterase (AChE)

Mental activity and the central cholinergic system are tightly linked. The principal neurotransmitter, acetylcholine (ACh), is involved in learning and memory acquisition in addition to its fundamental role in maintaining awareness. A notable reduction in ACh levels in the brain is associated with AD, which causes neurodegenerative symptoms to manifest. Additionally, increased acetylcholinesterase (AChE) production in the synaptic cleft destroys acetylcholine, which promotes the progression of AD [9]. Amyloid peptides also decrease the production of ACh, which is connected to the synthesis of Aβ. Nicotinic receptors may be directly stimulated by low concentrations of Aβ. Seven isoforms of nAchR may be activated by 100 pM of Aβ1-42. Modest doses of Aβ may block AchR. [10,11]. However, in high concentration, Aβ may cause a desensitization of its receptors while reducing the release of many neurotransmitters synaptically, convert amyloid precursor proteins into non-amyloid products and a decrease in amyloid formation and aggregation may be impacted by cholinergic receptor activation which lessens brain damage [12]. As a result, excessive ACHE production may unintentionally cause amyloid to develop, which has detrimental effects on the brain. Anti-AChE is the first-line medication used to treat AD symptoms as of now days.

2.2. Amyloid-Beta Hypothesis

Buildup of Aβ plaques in the brain is the primary cause of AD according to the amyloid cascade theory [13]. Regular clearing processes of Aβ are interfered, which causes Aβ to build up and deposition of Aβ plaques [14]. Aβ is a peptide that is produced when beta-secretase (β-secretase) or gamma-secretase (γ-secretase) proteolytically processes amyloid precursor protein (APP) in the brain tissues of AD patients [15]. There are different forms of Aβ peptides, and their prevalence determined by thier length. Aβ40 and Aβ42 are the most common forms, and Aβ42 is thought to be more toxic than Aβ40 and is more likely to aggregate and form Aβ plaques in brain tissues [16]. Aβ peptides are found in β-sheet conformation aggregates and polymerized plaques, where they generate in structurally distinct forms, such as polymorphic and fibrillar oligomers [17].

The build-up of Aβ protein initiates a sequence of events that culminate in the degeneration of nerve cells and impairment of brain tissue, ultimately culminating in the manifestation of AD symptoms. The amyloid cascade hypothesis postulates that the accumulation of Aβ sets off a series of neurodegenerative events, including oxidative stress, inflammation, and Tau protein accumulation, which in turn cause dementia symptoms. The amyloid cascade theory has sparked research into a number of possible AD treatment approaches, including immunotherapy to remove Aβ plaques from the brain and β-site amyloid precursor protein cleaving enzyme 1 (BACE1) inhibitors to target the BACE enzymes that produce Aβ. Despite being the most researched concept, the amyloid cascade theory falls short in explaining the complicated etiology of AD since other factors also play a role in the disease's progression [18, 19].

2.3. Tau Protein Hypothesis

One significant pathogenic characteristic of AD is the presence of intracellular tau-containing NFTs [20]. Paired helical filaments aggregate to form NFTs. The majority of hyperphosphorylated tau proteins are seen in pathological NFTs [21].

Tau proteins vary widely in molecular weight and are members of a family of microtubule-binding proteins. Tau plays a major role in stabilizing microtubules, and which is crucial for neurons since microtubules act as highways for the cargo that is transported in dendrites and axons [22]. The 352-residue tau protein is encoded by the cDNA, which was cloned and sequenced in 1988. Two large transcripts, measuring 6 and 2 kilobases in length and extensively dispersed across the brain, have been found by RNA blot analysis [23, 24]. Six tau isoforms are produced in humans by alternative splicing of the tau gene's exons 2, 3, and 10. Differential splicing of exon 10 results in tau species with repetitions of three arginines (3R) or four arginines (4R) that are microtubule-binding carboxyl terminals. For tau to avoid aggregating, an equimolar ratio of 3R and 4R could be crucial [25, 26].

The disease associated with tau typically starts off isolated and localized in the brain before expanding to other places [27]. Fibrillar and misfolded tau aggregates have the potential to proliferate across cells in a manner akin to prion propagation, ultimately permeating the brains of AD patients. Tau fragment, can function as an endopathogen both in vivo and in culture experiments [22].

2.4 Oxidative stress hypothesis

Humans produce reactive oxygen species (ROS) and reactive nitrogen species (RNS) in a variety of normal and aberrant processes. ROS and RNS serve a dual purpose in cellular signaling pathways and venomous processes that can damage cellular structures, such as cell membranes, lipids, proteins, and DNA. The brain is especially susceptible to oxidative stress due to its high oxygen consumption, which is 20% more than that of other mitochondrial respiratory tissues. The brain's fundamental functional unit, the neuron, is made up mostly of polyunsaturated fatty acids. It can combine

with ROS to trigger the lipid peroxidation process and molecular apoptosis. Another factor contributing to oxidative stress damage is reduced glutathione levels in neurons [28, 29].

2.5 Metal ion hypothesis

Metal dyshomeostasis has a role in the etiology and evolution of several illnesses, including as cancer and neurodegenerative disorders. Several compounds that are employed in therapeutic studies are recognized modulators of transition metal homeostasis, including metal chelators and ionosphere chelators. Not all medications that target transition metal homeostasis are metal-binding molecules [30]. Available evidence suggests that the balance of redox transition metals, namely iron (Fe), copper (Cu), and other trace metals, are elevated in AD. Cu, manganese, aluminum, and zinc are implicated in several neurodegenerative illnesses [31].

2.6 Inflammatory hypothesis

AD is also largely influenced by the inflammatory responses of astrocytes and microglia in the central nervous system (CNS) [32]. 10% to 15% of all brain cells are microglial cells, which are brain-specific macrophages in the central nervous system [33]. Compared to the control group, microglia cells in AD patients are more active. In AD patients, the density of aggregated microglial cells close to senile plaques and neurons with NFTs is typically two to five times greater than in healthy persons. Inflammation is also brought on by histocompatibility complexes and inflammatory factors that are produced by microglia.[34].

Aβ exhibits a synergistic impact on the activation of microglia produced by cytokines. It appears that Aβ's fibrillar structure is essential for *in vivo* glial activation [35]. Aβ can bind to microglia cells via the NLRP3 inflammatory complex and the CD36-TLR4-TLR6 receptor complex in AD patients. This can lead to cell destruction, the production of chemicals that induce inflammation, such as TNF-α, and immunological responses.

Apart from elevated TNF-α levels, elevated CNS concentrations of inflammatory cytokines such as IL-1β, TGF-β, IL-12, and IL-18 are also associated with the advancement of AD and worsen brain damage in AD patients [36]. B-cell receptor CD22 controls phagocytosis negatively. The overexpression of CD22 may lead to the functional decrease of aged microglia; hence, CD22 inhibition might improve the removal of debris and fibrils, including Aβ oligomers, *in vivo*, and this process may be advantageous for the treatment of AD [37, 38].

2.7 NMDA Hypothesis

Significant alterations in brain histology and behavior are hallmarks of AD. Intraneuronal NFTs and extracellular amyloid plaques are the two microscopically distinctive features of the AD brain Toxic effects of amyloid-beta (Aβ) on neurons, particularly in Alzheimer's disease, depend on the presence of tau protein. Furthermore, soluble forms of both Aβ and tau are thought to interact and cooperate in driving neurons towards a diseased state. This interaction is not solely dependent on the formation of plaques and tangles (the hallmark lesions of AD), but rather on the soluble, extracellular forms of these proteins [39]. The loss of cognitive function associated with AD is intimately linked to synaptic plasticity, where NMDAR is essential [40]. NMDAR-mediated excitatory glutamatergic neurotransmission is essential for both neuronal survival and synaptic plasticity. On the other hand, increased NMDAR activity induces excitotoxicity and encourages cell death, which may be the fundamental mechanism of AD neurodegeneration. Glutamate availability and NMDAR channel function modification are the two main variables influencing NMDAR signaling in AD [41].

3. *In-Vitro* methods for Screening of molecules

3.1 Acetylcholinesterase (AChE)

3.1.1 HPTLC bio-autography assay

For screening of molecules for AChE inhibition each molecule (10 mg/mL) was applied in duplicate to TLC plates using an aliquot (50 µL). Galantamine (1.0 mg/mL) was taken as a positive control. Following development, TLC plates were air-dried, and an AChE enzyme solution (6.7 U/mL in Buffer A) was sprayed over one plate until it was saturated. In order to measure the amount of enzyme activity present, 20 mL of Fast Blue salt (7.4 mM) in distilled water and 5 mL of 1-naphthyl acetate (13.4 mM) in ethanol were sprayed over the plate. Compounds that inhibit AChE are shown by white zones on a purple backdrop. And the second TLC plate was used as the reference plate for the isolation process after it was derivatized as directed using p-anisaldehyde [42, 43].

3.1.2 Microplate assay

The AChE inhibitory activity of the molecules was determined using a quantitative colorimetric method based on Ellman's method, with some modifications [44, 45]. A triplicate of a 96-well microplate was prepared with a 25 µL aliquot of 15 mM ATCI in water, 125 µL of 3 mM DTNB in Buffer B, 50 µL of Buffer and 25 µL of the test sample (1.0 mg/mL in 10% aqueous methanol). Absorbance was measured at 405nm, at every 15 seconds (five times), using a microplate reader. Following the addition of acetylcholinesterase (25 µL of 0.22 U/mL solution in Buffer A) to each well, the plate was mixed and allowed to set at room temperature for 10 minutes. At intervals of 15 seconds, the absorbance was measured eight more times. The sample's inhibition was compared to the blank (10% aqueous methanol) to determine the percentage of inhibition. The initial absorbance was deducted from the absorbance after the enzyme was added in order to prevent a rise in absorbance caused by the hydrolysis of the substrate. Serial dilutions of each test component were performed by transferring appropriate quantities of the mixture to create final test solutions with concentrations ranging from 200 µg/mL to 12.5 µg/mL in order to ascertain the IC50 values. Every assay was conducted twice, at various times. [46, 47].

3.2. Amyloid-Beta Hypothesis

3.2.1 Fluorescence resonance energy transfer (FRET)

The measure of inhibitory activity of compounds is based upon the reduction in the fluorescence quantum yield due to inhibition of BACE-1 enzymatic activity. The protease substrate (APP-based peptide) consists of a fluorescence donor (rhodamine) connected to a quenching acceptor through a peptide sequence (EVNLDAEFK). The fluorescence is weak intrinsically due to resonance energy transfer but upon enzymatic cleavage, the quantum yield of donor molecule increases. Inhibitory potential of the designed compounds can be governed from the reduced fluorescence quantum yield.

Initially, all of the substances were tested at a concentration of 25 µM. Compounds that demonstrated a percentage of inhibition ranging from 65.4 to 98.8% at 25 µM were retested at 100 µM, 50 µM, 10 µM, 5 µM, 1 µM, 0.5 µM, 0.1 µM, and 0.05 µM. The IC50 values were computed using the percentages of inhibition derived from the afore mentioned tests. Plotting the logarithmic concentration on the x-axis and the percentage of inhibition on the y-axis allowed for the calculation of the IC50 values [48, 49].

3.3 Tau Protein Hypothesis

3.3.1 Fibrillization assay

Rrecombinant myc-tagged truncated tau fragment K18, instead of K19, is used. [50] In order to compare the thioflavine T (ThT) fluorescence assay with antibody-based assays like the DELFIA and Alpha Screen, the myc tag was added. The ThT assay is preferred assay for the primary screening since it was generally easier to use and more repeatable than the antibody-based assays, especially when conducted under automated HTS settings. The reaction mixture contained 20 µM myc-tagged K18 (1:1: N-terminal myc:C-terminal myc tag), 20 µM heparin, and 2 mM DTT in 100 mM sodium acetate, pH 7.0. Prior to the fluorescence reading, 18 hours of incubation at 37° C were followed by the addition of 25 µl of a 25 µM solution of ThT and 1 hour of room temperature incubation. K18 in DMSO as positive control, and the non-fibrillizing mis-sense K18 mutant (K18-K311D), which was produced by replacing lysine 311 with aspartate was taken as a negative control [51].

In secondary assay, ThT reaction was sedimented at 186,000 g for 30 minutes using a 25% sucrose cushion, and the pellet's supernatant was extracted. A 12.5% acrylamide gel was used for SDS-PAGE analysis of the pellets after they had been resuspended in a volume equivalent to the supernatant. Myc-tagged K18 that was N-terminal and C-terminal moved quite differently and appeared as a double band. The resuspended sedimentation pellets were subjected to electron microscopy (EM) after negative staining with uranyl acetate [51].

3.4 Oxidative stress hypothesis

3.4.1 Oxygen radical absorbance capacity (ORAC-FL) assay

Phosphate buffer (75 mM, pH 7.4) was used to dilute the fluorescein (FL) stock solution and the tested chemical to 0.117 µM and 20 µM, respectively. The same buffer was used to dilute the (±)-6-hydroxy-2,5,7,8-tetramethylchroman-2-carboxylic acid (Trolox) solution to 100, 80, 60, 50, 40, 20, and 10 µM. Prior to the experiment, 108.4 mg of 2,20-azobis-(amidinopropane) dihydrochloride (AAPH) was dissolved to 40 mM in 10 mL of 75 mM phosphate buffer (pH 7.4). After pre-incubating the mixture containing the tested chemical (20 lL) and FL (120 µL; final concentration of 70 nM) at 37 °C for 10 minutes, 60 µL of the AAPH solution was added. For 120 minutes, the fluorescence was measured at 1-minute intervals (kexc = 485 nm; kem = 520 nm). The fluorescence readings were adjusted to match the blank's (antioxidant-free) curve [52].

3.5 Metal ion hypothesis

3.5.1 Inhibition and disaggregation of metal-induced Aβ1-42 aggregation

Metal-induced amyloid-beta (Aβ) aggregation, particularly with Aβ1-42, is a key process in Alzheimer's disease (AD) pathogenesis. Several strategies aim to inhibit this aggregation or even disaggregate pre-formed fibrils. These approaches involve using metal chelators, peptidomimetics, and other small molecules to disrupt the aggregation process and potentially reverse its effects. ThT was also used to assess the impact of inhibitors on metal-induced Aβ1-42 aggregation. Thioflavin T (ThT) is a benzothiazole salt used as a dye to visualize and quantify the presence or fibrilization of misfolded protein aggregates, or amyloid, both in vitro and in vivo. ThT binds to amyloid fibrils, increasing fluorescence. This assay is used to quantify the amount of fibrillar Aβ1-42 present, which allow to assess how well compounds inhibit fibril formation. The stock Aβ1-42 solution was diluted with 150 µM NaCl and 20 µM HEPES (pH 6.6). Stock solution of $CuCl_2$, FeNTA (10mM) was prepared using distilled water. A mixture of the inhibitor (20µL, 50µM for the iron sample; 75µM for the copper sample, final concentration), $CuCl_2$ or FeNTA (20 µL, 25 µM, final concentration), and the peptide (20 µL, 25 µM, final concentration) were incubated in the dark at 37ºC for 24 hours in order to perform the inhibition experiment. The peptide and metal ions were first incubated for 24 hours at 37 ºC in the dark, followed by the addition of the inhibitor and another 24 hours of incubation under the same conditions in order to disaggregate the self-induced Aβ1-42 aggregation. Following incubation, 20 µL of the sample was taken out and put into a black 96-well plate. It was then diluted with 50 µM gly-NaOH buffer (pH 8.5) that included 5 µM ThT to reach a final volume of 200 µL. The absorbance was measured at 450nm [53].

3.5.2 TEM Assay

Transmission electron microscopy (TEM) is used in Alzheimer's disease research to visualize and analyze the structure of amyloid-beta (Aβ) and tau protein aggregates, which are hallmarks of the disease. TEM allows to study the morphology, size, and arrangement

of these protein aggregates, providing insights into their role in disease development and progression. An 80 µM solution was obtained by dissolving Aβ1–42 peptide (Millipore) in 10 mM phosphate buffer (pH 7.4) at 4°C. At 37°C, Aβ1–42 was incubated with and without chemicals. Both Aβ1–42 and the compounds had final values of 20µM. Aliquots of 10 µL samples were put on a carbon-coated copper/rhodium grid at predetermined intervals. The grid was negatively stained with a 2% phosphomolybdic acid solution for one minute after being rinsed with water. The specimen was moved for analysis in a transmission electron microscope (JEOL JEM-1400) after the excess staining solution was drained off using filter paper [54].

3.5.3 Metal chelating assay

A metal chelating assay in Alzheimer's disease (AD) aims to assess a substance's ability to bind to metal ions, particularly those implicated in AD pathogenesis, like copper (Cu) and iron (Fe). This is done by measuring the reduction in free metal ions in a solution after the chelating agent is added. Using a UV-vis spectrophotometer chelating tests were conducted in DMSO and MOPS (3-morpholinopropanesulfonic acid) buffer (pH 7.4) for the molar ratio assay. Compounds absorption spectra were captured at room temperature in a 1 cm quartz cell, either by itself or in combination with several concentrations of FeNTA.

The metal chelation assay was carried out in DMSO and MOPS buffer to determine the pFe(III) values. A spectrofluorophotometer with an emission mode of excitation wavelength (435 nm) and emission wavelength from 440 nm to 550 nm was used. MOPS buffer was treated with Chelex 100 before use . First, the addition of FeNTA (2µM, 4ml, total volume) quenched the fluorescence of CP645 (6µM, 4ml, total volume), which was then recovered by the addition of compounds (60µM, 4ml), respectively. All of the samples' fluorescence was found after 48 hours. The equation fluorescence (%) =11.743 pFe(III)-169 can potentially be used to determine the relative fluorescence intensity of the compounds combined with CP645-Fe since the maximum fluorescence intensities of CP645 (6µM) and CP645-Fe complex (6µM: 2µM) were set at 100% and 0%, respectively. The values that are quoted are the average of three separate calculations [53, 55].

3.6 Inflammatory hypothesis

3.6.1 Assays of Inflammatory Mediators

Assays for inflammatory mediators in Alzheimer's disease (AD) often involve measuring the levels of specific proteins and cytokines in cerebrospinal fluid (CSF), blood, or brain tissue. These assays help to understand the role of inflammation in the disease process and potentially identify biomarkers for diagnosis and treatment. Techniques include immunoassays (ELISA, Luminex), qPCR for gene expression analysis, and histological analysis of brain tissue.

Solid phase Quantikine human immunoassay kits (R&D Systems) were used to measure IL-6 levels. The variation coefficient was intra-assay 3.0–3.5% and inter-assay 3.4–7.2% evaluations.

In a C1q ELISA (Complement component 1q Enzyme-Linked Immunosorbent Assay), purified C1q standards or conditioned medium samples are added to a plate pre-coated with a polyclonal anti-C1q antibody (in this case, DAKO antiserum). This allows the C1q in the sample to bind to the antibody on the plate, forming a "sandwich" complex. The amount of C1q bound can then be quantified using a detection antibody conjugated to an enzyme, followed by a substrate reaction that produces a measurable signal.

Purified C1q standard or conditioned medium samples were added to plates coated with polyclonal anti-C1q antiserum (DAKO) for C1q ELISAs, and the plates were then incubated for two hours at 25°C to allow for C1q capture. A 100 ml of 0.3 mg/ml monoclonal anti-C1q antibody (Quidel) was added in order to bind the captured C1q. To find binding, biotinylated anti-mouse IgG (Pierce, Rockford, IL) was used. Using successive dilutions of purified C1q standards, the specificity of the enzyme-linked immunosorbent assay (ELISA) procedures was confirmed. As low as 3–8 pg C1q/ml could be detected by the C1q ELISA, according to pilot experiments [56].

3.6.2 Enzyme immunoassay

The tissue of the hippocampus was used to extract free FAs (FFAs) and CSF samples using the LXA4 enzyme immunoassay. The brain tissues were gathered during a four-year period and kept at -80°C for an equivalent amount of time before being processed further. The CSF samples were gathered over a three-year period and kept at -80°C until they were processed further. Hippocampal samples were homogenized in ethanol using a pestle homogenizer before being centrifuged at 1500 g for 15 minutes in order to extract the tissue. After being collected, the supernatant was acidified to a pH of 3.5. Sep-Pak C18 columns were used to extract both these samples and the acidified CSF samples. In short, acidified samples were loaded right away after the columns had been equilibrated with methanol and ddH2O.

Methyl formate was used to elute bound FFAs, nitrogen gas was used to dry them off, and extraction buffer included with the LXA4 EIA kit was used to resuspend them. This kit was used to analyze LXA4, and in accordance with the manufacturer's recommendations, RvD1 was quantified using a RvD1 EIA kit (Cayman Chemical). An FFA assay kit (Cayman Chemical) was used to measure the total FFAs [57].

3.7 NMDA Hypothesis

3.7.1 Cell culture

Several cell culture assays can be used to investigate the N-methyl-D-aspartate (NMDA) receptor hypothesis for Alzheimer's disease (AD), which posits that excessive NMDA receptor activation (excitotoxicity) contributes to neuronal death. These assays typically involve exposing neurons to amyloid-beta (Aβ) oligomers, which are known to interact with and dysregulate NMDA receptors, and then measuring specific downstream effects.

Cell models for the assays

- **Primary neuronal cultures:** These are isolated directly from the hippocampus and cortex of rodents, the brain regions most affected by AD. They provide a highly relevant model for studying the effects of excitotoxicity.
- **Human induced pluripotent stem cell (hiPSC)-derived neurons:** These offer a human-specific model, allowing for studies using patient-derived cells. They are particularly valuable for studying genetic variations associated with AD.
- **Immortalized neuronal cell lines:** Cell lines like PC12 or mouse neuroblastoma (N2a) cells are easier to culture and are suitable for high-throughput screening. PC12 cells, for example, express NMDA receptors and can be used to study their function.

ECV304 is a cell line T24 bladder carcinoma cell line PBMEC medium was used to sustain cells at passages 145–190. IF medium (1:1 mixture of IMDM and Ham's F-12) with 7.5% (v/v) NCS, 7mM L-glutamine, 5 µg/mL transferrin, 0.5 U/mL heparin, 100 U/mL penicillin, 100 µg/mL streptomycin, and 0.25 µg/mL amphotericin B make up C6medium medium, to put it briefly [58].

Glioma C6 cells were cultured at passages 18 to 50 in 175 cm2 gelatine-coated tissue flasks (Greiner Bio-One GmbH, Frickenhausen, Germany) in C6 medium to create glioma conditioned medium. The German Cancer Research Center Heidelberg provided the rat C6 glioma cells that were isolated from rat gliomas. Every day, 25 mL of C6 culture supernatant was collected, kept at 4 °C, and used within a maximum of one month. Every three to five days, cells were subcultured by trypsination under culture conditions that were established at 96% humidity in an incubator with 5% CO2/95% air environment.

Using the T-RexTM method, HEK293 cells heterologously expressing a human NMDA receptor made up of the subunits NR1 and NR2A were produced as NMDAR positive control cells. NR1 expression was inducible, whereas NR2A expression was stable. Shortly after, the restriction site EcoRI was used to subclone the cDNA of the hNR1 subunit (which was obtained in bluescript from Dr. Shigetada Nakanishi of the Osaka Bioscience Institute) into the vector pcDNA4/TO (Invitrogen Life Science), and Hind III verified that the orientation was correct. The vector pcDNAI contained the cDNA of the NR2A subunit. One day prior to transfection, two million 293/T-Rex cells were plated into 100 mm diameter cell culture dishes and transfected using a calcium-phosphate mixture of 1 µg of NR1/pCDNA4/TO and 5 µg hNR2A/pcDNAI. Plates were divided 1:4 or 1:8 one day after transfection, and two days later, the antibiotics blasticidin (5 µg/mL) and zeocin (300 µg/mL) were added for selection.

Using cytotoxicity caused by 100 µg/mL tetracycline in cells cultured in 48-well plates and prevented by 0.5 mM ketamin, surviving cell clones were examined for NMDA receptor expression. Clone 29 was selected for further research, and the cells were given the designation HEK293/NR1NR2A. MEM Eagle EBSS with glutamine media supplemented with 10% FCS, 50 µg/mL gentamycin, 300 µg/mL zeocin, and 5 µg/mL blasticidin made up the medium used to further cultivate HEK293/NR1NR2A cells. To create higher NMDA receptor concentrations, 100 µg/mL of freshly dissolved tetracycline was administered to stimulate NR1 subunit expression [58, 59, 60]

3.7.2 Measurement of the intracellular calcium level

At a density of 50000 cells/cm2, ECV304 cells were seeded onto black 96-well plates coated with gelatine (1%) (Greiner BioOne, Germany). The cells were then cultivated in growth media in an incubator set at 37 °C with 5% CO2/95% air environment and 96% humidity. Every other day, the medium was switched out. Following seven days of development, the Ca2+ studies were conducted. The first step involved removing the themeium and washing the cell layers three times with HBSS (H8264, Sigma Aldrich). Next, 200 µL/well of 4 µM Fluo-3-AM dissolved in HBSS (H8264, Sigma Aldrich) containing Pluronic F127, 20 mM Hepes, 2.5 mM Probenecid, and 1% BSA with an adjusted pH of 7.4 was added to the cells. The Fluo-3-AM solution was discarded after the cells had been incubated for one hour at room temperature in the dark. They were then rinsed twice with HBSS, and 75 µL/well HBSS (H6648, Sigma Aldrich) containing 2 mMCaCl2, 20 mMHepes, 2.5 mM Probenecid, and 1%BSA (pH=7.4) was added. The cells were then incubated for 30 minutes at 37 °C. To equilibrate the temperature for the baseline and determine the start values F0, the 96-well plate was then placed in the plate reader (Tecan Genios Pro, Austria) and four cycles at 37 °C were measured twice (ex.-λ=485 nm, em.-λ=535 nm). At least 35 cycles were recorded to track the intracellular Ca2+ level over 40 minutes (F1 values) following the addition of 25 µL/well of 4-fold concentrated substances (dissolved in the same HBSS buffer used for the previous incubation stage and also containing 40 µM Glycin). Following the experiment, supernatants were disposed of and 100 µL/well of 1% Triton X-100 in HBSS (H8264, Sigma Aldrich) was added to the well to lyse the cells and measure the greatest amount of fluorescence that remained as a control for proper Fluo-3-AM loading. To account for cell self-fluorescence, the calculated fluorescence levels of cells that were not loaded with Fluo-3-AM were first deducted from those that were. After then, all values were tied to the values before substance addition (F0), which were set to 100%. At the conclusion of the experiment, control values (F1) were also adjusted to 100% and other data were connected to them in order to make it easier to compare treatment groups. Using the formula $Ca2+i=Kd*(F-Fmin)/(Fmax-F)$, intracellular calcium levels (Ca2+i) were determined in accordance with the manufacturer's instructions for Fluo-3-AM. At 37 °C, Kd for Fluo-3 was 894 nM. The average value of the negative control was used to define Fmin values. Fmax values as the mean value of the positive control for 2.5 mM BAPTA At the examined time points for every experiment, 10 µM ionomycin and F values reflected the results of the control or with the addition of an NMDAR modulator. The Ca2+i values that were obtained after 40 minutes

(F1) were also set to 100%, and they were associated with other results. Before seeding 70000 cells/cm2 in growth media containing tetracycline and 0.5 mM ketamin, black 96-well plates were precoated with 25 µg/mL poly-D-lysine in the case of HEK293/NR1NR2A cells. Following Fluo-3-AM loading, tetracycline and ketamin-free buffers were utilized. The third day following sowing was when the experiments were conducted [58, 59].

3.7.3 Transendothelial electrical resistance studies

ECV304 cells were cultivated in growth medium at 37 °C, 95% air environment, 5% CO2/95% humidity, and a density of 80000 cells/cm2 on collagen (0.14 mg/mL) coated 6-well inserts (1 µmpore size, BD). Every other day, the medium (2 mL apical, 3 mL basolateral) was switched out. Growth inserts were utilized for transendothelial electrical resistance (TEER) tests after 14 days. Chopstick electrodes (Millipore) were used to measure TEER after one hour at room temperature in order to verify adequate tightness for the further investigation. After that, the wells and medium inserts were taken out and given two PBS washes. The cells were then given serum and heparin-free C6 media, and they were allowed to equilibrate for 30 minutes. In the instance of MK801, it had previously been preincubated in the experimental medium. Following the measurement of TEER (= initial values), drugs were added to serum, and after three hours, TEER was recorded in heparin-free C6 medium. Following the removal of the medium, inserts and wells were thoroughly cleaned with PBS twice to get rid of any remaining materials and new serum. Heparin-free C6 medium was then reintroduced for a further 21 hours. The medium was removed 24 hours after the last TEER data were recorded [58, 61].

4. Conclusion

Alzheimer's disease is complex and neurodegenerative disorder which is interconnected with pathological pathways such as cholinergic dysfunction, amyloid-beta aggregation, tau hyperphosphorylation, oxidative stress, metal ion imbalance, neuroinflammation, and NMDA receptor-mediated excitotoxicity. The innovative strategies are most needed for discover to effective disease-modifying therapies.

In the review highlights the in vitro screening methos for the identification and evaluations of potential anti-Alzheimer's agents. An inclusive biochemical and cell-based assays for the acetylcholinesterase inhibition, β-secretase activity, tau aggregation, antioxidant capacity, metal chelation, and inflammatory mediator assays to provide valuable insights into the mechanisms of action of newly develop molecules. Additionally, advanced cellular models like rimary neurons, human iPSC-derived neurons, and engineered cell lines to provide physiologically applicable to study neurotoxicity, neuroprotection, and receptor modulation, particularly in the context of NMDA receptor signaling.

Importantly, a promising therapeutic approach for AD is recognized by multiple assays for enables the identification of multi-target-directed ligands. Future research should be focus on in vitro study for the newly develop molecules incorporating human-relevant systems and the bridging the gap between preclinical findings and clinical outcomes. Overall, these in vitro screening methods are crucial for accelerating the development of effective and targeted therapies for Alzheimer's disease.

5. REFERENCES

6. Querfurth, H.; LaFerla, F. Alzheimer's Disease. N. Engl. J. Med. 2010, 362, 329–344.
7. Meldolesi, J. Alzheimer's disease: Key developments support promising perspectives for therapy. Pharmacol. Res. 2019, 146, 104316.
8. Cao, J.; Hou, J.; Ping, J.; Cai, D. Advances in developing novel therapeutic strategies for Alzheimer's disease. Mol. Neurodegener. 2018, 13, 64.
9. Kulshreshtha, A.; Piplani, P. Current pharmacotherapy and putative disease-modifying therapy for Alzheimer's disease. Neurol. Sci. 2016, 37, 1403–1435.
10. Jeffrey Cummings, Yadi Zhou, Garam Lee, Kate Zhong, Jorge Fonseca, Feixiong Cheng, Alzheimer's disease drug development pipeline: 2024, Alzheimer's Association, 2024, 10:e12465.
11. R. T. Bartus, R. L. Dean 3rd, B. Beer and A. S. Lippa, Science, 1982, 217(4558), 408–414.
12. R. Schliebs and T. Arendt, Behav. Brain Res., 2011, 221, 555–563.
13. Zhidong Liu, Aihua Zhang, Hui Sun, Ying Han, Ling Konga and Xijun Wang, Two decades of new drug discovery and development for Alzheimer's disease, RSC Advances, 2017, 7, 6046–6058.
14. Chen Ma, Fenfang Hong and Shulong Yang, Amyloidosis in Alzheimer's Disease: Pathogeny, Etiology, and Related Therapeutic Directions, Molecules, 2022, 27, 1210.
15. Dougherty, J.J.;Wu, J.; Nichols, R.A. Beta-amyloid regulation of presynaptic nicotinic receptors in rat hippocampus and neocortex. J. Neurosci. 2003, 23, 6740–6747.
16. Dineley, K.T.; Bell, K.A.; Bui, D.; Sweatt, J.D. beta-Amyloid peptide activates alpha 7 nicotinic acetylcholine receptors expressed in Xenopus oocytes. J. Biol. Chem. 2002, 277, 25056–25061.
17. Govoni, S.; Mura, E.; Preda, S.; Racchi, M.; Lanni, C.; Grilli, M.; Zappettini, S.; Salamone, A.; Olivero, G.; Pittaluga, A.; et al. Dangerous liaisons between beta-amyloid and cholinergic neurotransmission. Curr. Pharm. Des. 2014, 20, 2525–2538.
18. Chen GF, Xu TH, Yan Y, Zhou YR, Jiang Y, Melcher K, et al. (2017). Amyloid beta: structure, biology and structure-based therapeutic development. Acta Pharmacol Sin, 38:1205-1235.
19. Selkoe DJ (2001). Alzheimer's disease results from the cerebral accumulation and cytotoxicity of amyloid beta-protein. J Alzheimer's Dis, 3:75-80.
20. Storey E, Cappai R (1999). The amyloid precursor protein of Alzheimer's disease and the Abeta peptide. Neuropathol Appl Neurobiol, 25:81-97.

21. Walsh DM, Selkoe DJ (2007). A beta oligomers - a decade of discovery. J Neurochem, 101:1172-1184.

22. Selkoe DJ (1994). Alzheimer's disease: a central role for amyloid. J Neuropathol Exp Neurol, 53:438-447.

23. Evin G (2016). Future therapeutics in Alzheimer's disease: development status of BACE inhibitors. BioDrugs, 30:173-194.

24. Hirak Shah, Ashish Patel, Vruti Parikh, Afzal Nagani, Bhargav Bhimani, Umang Shah, Tushar Bambharoliya (2020). The β-Secretase Enzyme BACE1: A Biochemical Enigma for Alzheimer's Disease, CNS & Neurological Disorders-Drug Targets, 19(3): 184-194.

25. Braak, E. et al. Neuropathology of Alzheimer's disease: what is new since A. Alzheimer? Eur. Arch. Psychiatry Clin. Neurosci. 249(Suppl 3), 14–22 (1999).

26. Grundke-Iqbal, I. et al. Microtubule-associated protein tau. A component of Alzheimer paired helical filaments. J. Biol. Chem. 261, 6084–6089 (1986).

27. Clavaguera, F. et al. Transmission and spreading of tauopathy in transgenic mouse brain. Nat. Cell Biol. 11, 909–913 (2009).

28. Goedert, M., Wischik, C. M., Crowther, R. A., Walker, J. E. & Klug, A. Cloning and sequencing of the cDNA encoding a core protein of the paired helical filament of Alzheimer disease: identification as the microtubule-associated protein tau. Proc. Natl Acad. Sci. USA 85, 4051–4055 (1988).

29. Lee, G., Cowan, N. & Kirschner, M. The primary structure and heterogeneity of tau protein from mouse brain. Science 239, 285–288 (1988).

30. Andreadis, A., Brown, W. M. & Kosik, K. S. Structure and novel exons of the human tau gene. Biochemistry 31, 10626–10633 (1992).

31. Adams, S. J., DeTure, M. A., McBride, M., Dickson, D. W. & Petrucelli, L. Three repeat isoforms of tau inhibit assembly of four repeat tau filaments. PloS ONE 5, e10810 (2010).

32. Frost, B., Jacks, R. L. & Diamond, M. I. Propagation of tau misfolding from the outside to the inside of a cell. J. Biol. Chem. 284, 12845–12852 (2009).

33. Liu Z, Zhang A, Sun H, et al. Two decades of new drug discovery and development for Alzheimer's disease. RSC Advances. 7(10), 6046–6058 (2017).

34. Ajit K. T., Parul K., Kritika G., Karan A. Pathophysiology and management of alzheimer's disease: an overview. Journal of Analytical & Pharmaceutical Research. 7(2), 226–235 (2018).

35. Weekley CM, He C. Developing drugs targeting transition metal homeostasis. Curr Opin Chem Biol. 37, 26–32 (2017).

36. Prakash A, Dhaliwal GK, Kumar P, et al. Brain biometals and Alzheimer's disease – boon or bane? Int J Neurosci. 127(2), 99–108 (2017).

37. Bagyinszky, E. et al. Role of inflammatory molecules in the Alzheimer's disease progression and diagnosis. J. Neurological Sci. 376, 242–254 (2017).

38. Santos, L. E., Beckman, D. & Ferreira, S. T. Microglial dysfunction connects depression and Alzheimer's disease. Brain Behav. Immun. 55, 151–165 (2016).

39. McGeer, E. G. & McGeer, P. L. Neuroinflammation in Alzheimer's disease and mild cognitive impairment: a field in its infancy. J. Alzheimer's. Dis. 19, 355–361 (2010).

40. Eikelenboom, P. & Stam, F. C. Immunoglobulins and complement factors in senile plaques. An immunoperoxidase study. Acta Neuropathol. 57, 239–242 (1982).

41. Michaud, M. et al. Proinflammatory cytokines, aging, and age-related diseases. J. Am. Med. Dir. Assoc. 14, 877–882 (2013).

42. Pluvinage, J. V. et al. CD22 blockade restores homeostatic microglial phagocytosis in ageing brains. Nature 568, 187–192 (2019).

43. Pei-Pei L., Yi X., Xiao-Yan M. and Jian-Sheng K. History and progress of hypotheses and clinical trials for Alzheimer's disease. Nature. 4(1), 1-22 (2019).

44. Bloom, G. S. (2014). Amyloid-b and tau. JAMA Neurol. 71:505. doi: 10.1001/jamaneurol.2013.5847

45. Parameshwaran, K., Dhanasekaran, M., and Suppiramaniam, V. (2008). Amyloid beta peptides and glutamatergic synaptic dysregulation. Exp. Neurol. 210, 7–13. doi: 10.1016/j.expneurol.2007.10.008

46. Wang, R., and Reddy, P. H. (2017). Role of glutamate and NMDA receptors in Alzheimer's disease. J. Alzheimer's Dis. 57, 1041–1048. doi: 10.3233/JAD-160763.

A. Marston, J. Kissling, K. Hostettman, A rapid TLC bioautographic method for the detection of acetylcholinesterase and butyrylcholinesterase inhibitors in plants, Phytochem. Anal. 13 (2002) 51–54.

47. H.R. Adhami, J. Lutz, H. Kahlig, M. Zehl, L. Krenn, Compounds from gum ammoniacum with acetylcholinesterase inhibitory activity, Sci. Pharm. 81 (3) (2013) 793–805.

48. I.K. Rhee, M. van de Meent, K. Ingkaninan, R. Verpoorte, Screening for acetylcholinesterase inhibitors from Amaryllidaceae using silica gel thin-layer chromatography in combination with bioactivity staining, J. Chromatogr. A 915 (2001) 217–223.

49. K.L. Vegad, E.D. Patel N.S. Kanaki, Enzyme Activity Guided Isolation of Nardostachys jatamansi for Acetylcholinesterase Inhibitory Activity, Inventi Impact: Ethnopharmacology, (1) 2017:18-21.

50. N. Cortes, R. Alvarez, E.H. Osorio, F. Alzate, S. Berkov, E. Osorio, Alkaloid metabolite profiles by GC/MS and acetylcholinesterase inhibitory activities with binding-mode predictions of five Amaryllidaceae plants, J. Pharm. Biomed. Anal. 102 (2015) 222–228.

51. P. Jain, P. K. Wadhwa, S. Gunapati, H. R. Jadhav, Design, synthesis and in vitro evaluation studies of sulfonyl-amino-acetamides as small molecule BACE-1 inhibitors, Bioorg. Med. Chem. 24(11) (2016) 2567-2575.

52. K.L. Vegad, N.S. Kanaki, M.N. Zaveri, E.D.Patel, Bio Activity Guided Separation of Acetyl cholinesterase Inhibitor from Nardostachys jatamansi, International Journal of Medicine and Pharmaceutical Research 3 (4), 1076–1079.

53. V. Bhasker, R. Chowdary, S. R. Dixit, S. D. Joshi, Synthesis, molecular modeling and BACE1 inhibitory study of tetrahydrobenzo[*b*] pyran derivatives, Bioorg. Chem. 84 (2019) 202-210.

54. M. Pickhardt, Z. Gazova, M. von Bergen, I. Khlistunova, Y. Wang, A. Hascher, E.M. Mandelkow, J. Biernat, E. Mandelkow, Anthraquinones inhibit tau aggregation and dissolve Alzheimer's paired helical filaments in vitro and in cells, J. Biol. Chem. 280 (5) (2005) 3628–3635.

55. Crowe, A., Ballatore, C., Hyde, E., Trojanowski, J.Q., Lee, V.M.Y., 2007. High throughput screening for small molecule inhibitors of heparin-induced tau fibril formation. Biochem. Biophys. Res. Commun. 3s58, 1–6.

56. Shishun Xie, Jie Chen, Xiruo Li, Tao Su, Yali Wang, Zhiren Wang, Ling Huang, Xingshu Li, Synthesis and evaluation of selKunjegiline derivatives as monoamine oxidase inhibitor, antioxidant and metal chelator against Alzheimer's disease, Bioorganic & Medicinal Chemistry. 23(13), 2015, 3722-3729.

57. Ping Xu, Minkui Zhang, Rong Sheng, Yongmin Ma, Synthesis and biological evaluation of deferiprone-resveratrol hybrids as antioxidants, Aβ1–42 aggregation inhibitors and metal-chelating agents for Alzheimer's disease, European Journal of Medicinal Chemistry. 127, 2017, 174-186.

58. L. Huang, C. Lu, Y. Sun, F. Mao, Z. Luo, T. Su, H. Jiang, W. Shan, X. Li, Multitarget-directed benzylideneindanone derivatives: anti-beta-amyloid (Abeta) aggregation, antioxidant, metal chelation, and monoamine oxidase B (MAO-B) inhibition properties against Alzheimer's disease, J. Med. Chem, 55 (2012) 8483-8492.

59. Y. Ma, W. Luo, P.J. Quinn, Z. Liu, R.C. Hider, Design, synthesis, physicochemical properties, and evaluation of novel iron chelators with fluorescent sensors, J. Med. Chem, 47 (2004) 6349-6362.

60. Lih-Fen Lue, Russell Rydel, Elizabeth F. Brigham, Li-Bang Yang, Harald Hampel, Greer M. Murphy, Jr., Libuse Brachova,1 Shi-Du Yan, Douglas G. Walker, Yong Shen, And Joseph Roger, Inflammatory Repertoire of Alzheimer's Disease and Nondemented Elderly Microglia In Vitro, Wiley-Liss, 35, (2001) 72–79.

61. Hardy J & Selkoe DJ, The Amyloid Hypothesis of Alzheimer's Disease: Progress and Problems, *Science* (2002), 297 (5580), 353-356.

62. Xiuzhe Wang, Mingqin Zhu, Erik Hjorth, Veronica Cortes-Toro, Helga Eyjolfsdottir, Caroline Graff, Inger Nennesmo, Jan Palmblad, Maria Eriksdotter, Kumar Sambamurti, Jonathan M. Fitzgerald, Charles N. Serhan, Ann-Charlotte Granholm, Marianne Schultzberg, Resolution of inflammation is altered in Alzheimer's disease, Alzheimer's & Dementia, 11(1), 2015, 40-50.

63. Neuhaus, W., Noe, C.R., 2009. Transport at the blood–brain barrier. In: Ecker, G., Chiba, P. (Eds.), Transporters as Drug Carriers: Structure, Function, Substrates: 44 (Methods and Principles in Medicinal Chemistry). Wiley-VCH Verlag GmbH & Co. KGaA, Weinheim, Germany, pp. 263–298.

64. Sommerauer, C., 2010. Molecular pharmacology of amantadine and related substances in cells heterologously expressing human transporters and receptors. Master thesis, Medical University of Vienna, Brain Research Center.

65. Winfried Neuhausa, Michael Freidl, Phillip Szkokan, Michael Berger, Michael Wirth, Johannes Winkler, Franz Gabor, Christian Pifl, Christian R. Noe, Effects of NMDA receptor modulators on a blood–brain barrier in vitro model, Brain Research, 1394, (2011), 49–61.